

# A Frequency Filter of Backscattered Light of Stimulated Raman Scattering due to the Raman Rescattering in the Gas-filled Hohlräume

Liang Hao,<sup>1</sup> Wenyi Huo\*,<sup>1</sup> Zhanjun Liu†,<sup>1</sup> Chunyang Zheng,<sup>1</sup> and Chuang Ren<sup>2,3</sup>

<sup>1</sup>*Institute of Applied Physics and Computational Mathematics, Beijing, 100094, China*

<sup>2</sup>*Department of Mechanical Engineering and Laboratory for Laser Energetics,  
University of Rochester, Rochester, New York 14627, USA*

<sup>3</sup>*Department of Physics and Astronomy,  
University of Rochester, Rochester, New York 14627, USA*

(Dated: April 26, 2019)

## Abstract

The coupling evolutions of stimulated Raman scattering (SRS) and Raman rescattering (re-SRS) are studied under the parameter conditions of relevance to the gas-filled hohlraum experiments at the National Ignition Facility by a nonenveloped fluid code for the first time. It is found that re-SRS works as a frequency filter of backscattered light of SRS in the gas region. The low frequency modes originated from density points higher than about  $0.1n_c$  would stimulate re-SRS and be heavily depleted by re-SRS at the region of their effective quarter critical density region. Due to the high collisional damping of the rescattered light, the energy of rescattered light is deposited quickly into the plasmas along with its propagation, which limits the re-SRS in a small region. Large amplitude of the daughter Langmuir wave of re-SRS would stimulate cascade Langmuir decay instabilities and induce obvious low frequency density modulations, which can further result in the inflation of high frequency modes generated at density points lower than the growth region of re-SRS.

PACS numbers: 52.50Gi, 52.65.Rr, 52.38.Kd

---

\* Email: huo\_wenyi@iapcm.ac.cn

† Email: liuzj@iapcm.ac.cn

Laser plasma instabilities (LPIs) [1], such as stimulated Raman scattering (SRS), stimulated Brillouin scattering (SBS), are of great importance in laser driven inertial confinement fusions. In direct drive inertial confinement fusion, SRS and SBS can reduce the laser absorption. SRS would generate energetic electrons which may preheat the fuel. SBS would result in cross beam energy transfer (CBET) between overlapped laser beams and drive asymmetry [2, 3]. In indirect drive inertial confinement fusion, SRS and SBS would scatter the laser energy out of hohlraums which are used to convert laser energy into soft X rays. As a result, SRS and SBS lead to the reduction of the laser energy absorbed by the hohlraum wall and the conversion efficiency from laser into soft X rays. The CBET would redistribute the laser deposition and result in drive asymmetry [4–6]. Besides, SRS and two plasmon decay are important sources of energetic electrons in both direct and indirect drives [7].

Generally, indirect drive inertial confinement fusion uses gas-filled hohlraums to mitigate the flow of wall and ablator plasmas into the interior of the hohlraum [8–10]. In the past years, there have been many works engaged in the study of LPIs in the gas-filled hohlraums [11–17]. These works mainly concentrate on the primary LPIs mentioned above, based on the linear ray-racing model [12, 13], enveloped fluid model [14–16], or kinetic simulation [17]. However, the experimental results at the National Ignition Facility (NIF) indicate that the LPIs in the gas-filled hohlraums are too complicated and difficult to be well understood. For example, the SRS level of the laser beam at  $30^\circ$  seems to be saturated and do not go up with the transferred energy from outer cones by CBET [18], and the wavelength of SRS backscattered light is commonly shorter than simulations of the linear ray-tracing code [12, 13]. A lack of understanding and controlling LPIs is believed to be one of major contributors to the failure to achieve ignition [19].

In fact, besides the primary LPIs, some secondary LPIs, such as the Langmuir decay instability (LDI) [20], and the rescattering of the scattered light of the primary LPIs, including Raman rescattering (re-SRS) [21], Brillouin rescattering [22], and the two plasmon decay [23], may also play an important role in the gas-filled hohlraums. Using particle-in-cell simulations, Hinkel *et al.* pointed out that the rescattering could appear in the NIF hohlraums [21], and the rescattering of SRS was found to be one of the important sources of energetic electrons with energy higher than 100 keV [24]. In this Letter, we studied the coupling evolution of SRS and re-SRS with nonenveloped fluid code in the indirect drive regime for the first time. It is found that the re-SRS, which is not only one of the nonlinear

saturation mechanism of SRS stimulated from the high density region, but also can induce the inflation of SRS generated in the low density region, can work as a frequency filter of backscattered light of SRS. The results explain why the observed light wavelength of SRS is shorter than the linear simulations for the inner laser cones in the NIF gas-filled hohlraum experiment. In addition, our study can partially explain the “energy deficit” appeared in the gas-filled hohlraum experiments at the NIF [25].

Commonly, in gas-filled hohlraum experiments at the NIF, there is a large inhomogeneous plasma region in gas with the maximum electron density higher than  $0.1n_c$ , where  $n_c$  is the critical density. Theoretically, the scattered light of convective backward SRS (BSRS) can stimulate re-SRS below the density points  $0.11n_c$ . In order to explore the possible coupling between BSRS and re-SRS in experiments, in this study, we mainly focus on the inhomogeneous linear density profile ranged from  $0.08 n_c$  to  $0.11 n_c$  with a large scale length of about 2 mm, which is similar to the plasma conditions in the NIF gas-filled hohlraums [12, 26]. The pump laser wavelength  $\lambda_0$  is  $0.351 \mu\text{m}$ , and ion species is ionized Helium, which are typically used in ICF experiments. Temperatures are  $T_e = 1.5 \text{ keV}$  for electrons and  $T_i = 1 \text{ keV}$  for ions. So the production of the wavenumber of Langmuir wave (LW)  $k_L$  and the Debye length  $\lambda_D$  maintained smaller than 0.3 for both SRS and re-SRS, where the kinetic effects are not important in the fluid regime. Two one-dimensional simulations with fixed and mobile ions were done with FLAME code, which is a fluid code based on the full wave equations for vector potentials of light without any envelope approximations and can cover the coupling evolution of SRS, SBS, LDI, and rescattering inherently in the inhomogeneous plasma [27]. Seed level can be controlled in this code, which avoids the impacts of high artificial noises on LPs which often appears in Particle-in-Cell simulations [28, 29]. Currently, in order to ensure the reasonable collisional damping rates for the light signals with different frequencies, we have improved the code by substituting the quiver velocity  $v_{\alpha,\beta}$  for the vector potential  $A_{\alpha,\beta}$  in the right hand side coupling terms of the electron and ion momentum equations and replacing the original equations of vector potential by  $(\partial^2/\partial t^2 - \partial^2/\partial x^2) A_\alpha = -n_L v_\beta - n_A v_\alpha$  combined with  $(\partial/\partial t + \nu_{ei}) v_\alpha = \partial A_\alpha/\partial t$ , where subscripts  $\alpha, \beta = 0$  or  $1$ , and  $\nu_{ei}$  is the electron-ion collisional damping rate [27]. In the simulations, the length of entire simulation box is  $16800 c/\omega_0$ , including the physical domain  $L = 12000 c/\omega_0$  (about  $670 \mu\text{m}$ ) and two perfect matched layers [30] of  $L_{lay} = 2400 c/\omega_0$  each at the left and right boundaries, which are used to ensure a good absorption of signals out

of the physical boundaries. The magnitude of volume noises is  $10^{-9} n_c$  in order to describe the thermal noises [31]. And each simulation is ran about 40 ps with laser intensity  $I_0 = 2 \times 10^{15} \text{ W/cm}^2$ .

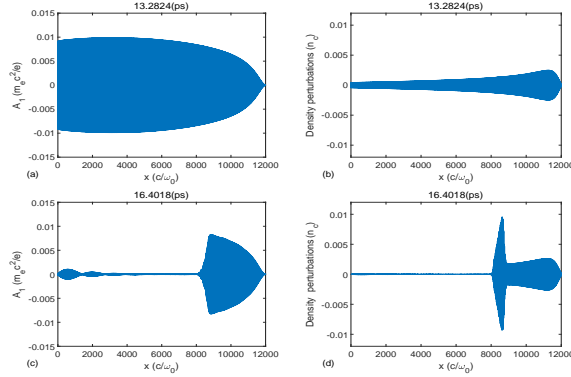


FIG. 1: (Color online) Snapshots of (a,c) vector potential of SRS scattered light and (b,d) high frequency density perturbations due to the LWs of SRS and re-SRS at about (a,b) 13.3ps and (c,d) 16.4ps for the fixed ions case.

In order to show the process of re-SRS clearly, we first investigate the case with fixed ions. The vector potential of SRS scattered light  $A_1$  and the high frequency electron density perturbations of LWs are shown in Fig. 1. The spectra of light waves and LWs in  $\omega - k$  space are shown in Fig.2, which are obtained in the region of  $8200-8800c/\omega_0$  (the density is  $0.1005-0.102n_c$ ) by using the 2-dimensional Fourier transform. Signals on the left half side with ( $k < 0$ ) and on the right half side with ( $k > 0$ ) represent the waves propagating forward to the right and propagating backward to the left in real space, respectively.

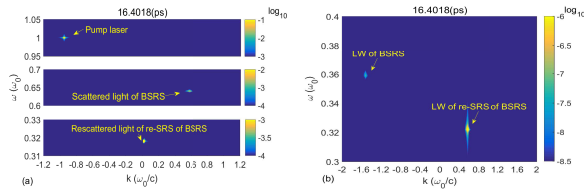


FIG. 2: (Color online)  $\omega - k$  space of (a) light wave and (b) LWs of BSRS and re-SRS in the range of  $8200-8800c/\omega_0$  at the time about 16.4ps for the fixed ions case.

As shown in Figs. 1(a) and 1(b), the convective BSRS rise firstly near the right boundary before the growth of re-SRS, because the temporal growth rate of BSRS is commonly larger at higher density. Scattered light of BSRS with the frequency about  $\omega_R = 0.64 \omega_0$  propagates

from right to left and is amplified along with its propagation, accompanied with the growth of LW on its path. Both light wave and LW show the feature of the single mode in whole physical domain, which indicates that BSRS is much easier to be stimulated by the seed light originated from high density region than the local thermal noises in the low density region. However, the convective amplification of scattered light became slower in the left side due to the detune induced by the density gradient. In the region of  $8200 - 8800 c/\omega_0$ , the density is just close to the effective quarter critical density of the scattered light of BSRS, so absolute mode of re-SRS is easy to be stimulated. As shown in Figs. 1(c) and 1(d), re-SRS rise clearly in this special region, and the scattered light of BSRS was strongly depleted by re-SRS. Judging from the spectra shown in Fig. 2, both the rescattered light and the LW of re-SRS propagates backward to the left side. And re-SRS grew rapidly to a large level in a small region and then decreased quickly along the propagation of its daughter waves as shown in Figs. 1(d). According to the matching condition of re-SRS, the frequency and wavenumber of the rescattered light are  $0.318 \omega_0$  and  $0.005 \omega_0/c$  respectively at the effective quarter critical density of the backscattered light of BSRS, while the frequency and wavenumber of the backward LW of re-SRS are  $0.322 \omega_0$  and  $0.54 \omega_0/c$  respectively, which are consistent with the corresponding modes as shown in Fig. 2. Due to the small  $k_L \lambda_D$  of the LW of re-SRS, which is only about 0.1 here, Landau damping of LW of re-SRS is very small. However, the collisional damping of rescattered light is about 10 times higher than the incident light because the frequency of rescattered light is very low. So the collisional damping, which dominated over the Landau damping here, is the main reason for the threshold of re-SRS and the quick damping of its daughter waves in space. Another reason for the saturation of re-SRS is the depletion of the scattered light of BSRS. Fig. 3 shows the reflectivity of scattered light and rescattered light, which is diagnosed in  $\omega - k$  space at the left boundary of physical domain through 2-dimensional Fourier transform. In the fixed ions case, reflectivity of backscattered light of BSRS reached its maximum saturated level of about 24.3 % firstly and then largely decreased from about 16 ps accompanied with the growth of re-SRS. After the enough growth of re-SRS, SRS and re-SRS evolves to a steady state finally, and most of the energy in scattered light of BSRS was transferred into the daughter waves of re-SRS and then deposited in plasma due to the collisional damping. Temporal-averaged reflectivity of scattered light of BSRS and rescattered light of re-SRS were 1.7% and 0.05%. No forward SRS was observed because of the density gradient [24].

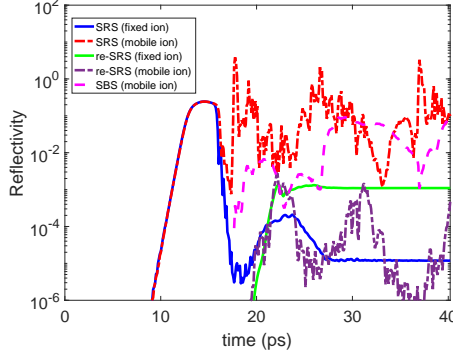


FIG. 3: (Color online) Reflectivity of backward scattered light at the left boundary versus time.

In order to be more closer to the real plasma condition in the gas-filled hohlraum experiments, we considered the case with mobile ions. As shown in Fig. 3, it is interested that the reflectivity of scattered light of BSRS decreases firstly at 16 ps and then increases quickly again to a higher saturated level, and strong bursts are presented. The temporal-averaged reflectivity of scattered light of BSRS and rescattered light of re-SRS are 13.3 % and 0.01%, respectively. Besides, some observable reflectivity of scattered light of backward SBS appears from about 17.5 ps, with the temporal-averaged value of 1.5 %. The key difference with the first simulation is that some low frequency density modulations of ion-acoustic waves (IAWs) occur in the region of  $8200 - 8800 c/\omega_0$ , accompanied with the growth of re-SRS. The spectra of LWs in  $\omega - k$  space at the time about 16.4 ps is shown in Fig. 4(a). In the left half part, besides the LW of BSRS with frequencies around  $0.36 \omega_0$ , there are some new modes with frequencies around  $0.32 \omega_0$ . These modes are the forward daughter LW of LDI. In order to confirm the existence and origin of LDI, the spectra of low frequency density modulations in this region is shown in Fig. 4(b). Obviously, there are some modes of IAWs with frequency around  $0.001 \omega_0$  and the wavenumber around  $1.1 \omega_0/c$ , which is about two times of the wavenumber of the backward LW of re-SRS but not the forward LW of BSRS. Therefore, the low frequency density modulations in this region originates from LDI, which is stimulated by the backward LW of re-SRS. According to matching condition of LDI, the modes of IAW in right half side is the backward daughter IAW of LDI, and the modes in the left half side indicate the cascade LDI induced by the forward daughter LW of LDI as labeled in Fig. 4(b).

In Fig. 5(a), we show the scattered light of BSRS at about 16.4 ps. Similar to the fixed

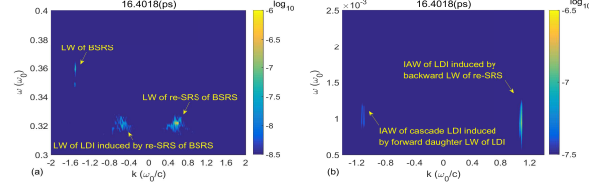


FIG. 4: (Color online)  $\omega - k$  space of (a) LWs of SRS, re-SRS and LDI, and (b) IAWs of cascade LDI in the range of  $8200-8800c/\omega_0$  at the time about  $16.4\text{ps}$  for the mobile ions case.

ions case shown in Fig. 1 (c), the scattered light of BSRS is strongly depleted in the region of  $8200 - 8800 c/\omega_0$  due to re-SRS. However, it is re-borned at the left side of this region. Fig. 5(b) shows the scattered light of BSRS at a later time  $17.5 \text{ ps}$ , in which the front part of the re-borned backscattered light is amplified convectively to a much higher level than its saturated level before the growth of re-SRS as shown in Fig. 1(a). We traced the convective inflated front part of the re-borned scattered light of BSRS, and gave its  $\omega - k$  spectra in the range of  $7000 - 7600 c/\omega_0$  and  $600 - 1200 c/\omega_0$  at  $16.4 \text{ ps}$  and  $17.5 \text{ ps}$  in Figs. 5(c) and 5(d), respectively. Compared with the single mode in Fig. 2(a), some modes of frequencies higher than  $0.64 \omega_0$ , which corresponds to the best matching modes of BSRS at different low density points, become stronger and stronger along with the backward propagation. Based on these features, the reason for the inflated BSRS is concluded as follow. First, re-SRS is stimulated by the low frequency modes of backscattered light originated from the high density region and induces LDI and even cascade LDI in the region of  $8200 - 8800 c/\omega_0$ . Second, the low frequency density modulations of LDIs generate some modes of scattered light of BSRS in a wider range of frequency locally in this special region. These modes could even be the local absolute modes when laser intensity was enough higher than the threshold [32]. Third, different frequencies of these modes could fulfill the best matching condition of BSRS at different low density points as they propagate to the low density region. So these modes finally work as a band of seeds and resulted in the amplification of the engine modes for different low density points together on the ray path.

In the experiments with gas-filled hohlraums at NIF, the wavelength of scattered light of BSRS is generally shorter than the simulation which is based on the linear ray-tracing model [12, 13]. Here we present an explicit explanation by investigating the coupling BSRS and re-SRS. Commonly, electron density grows like a continuous exponential function of distance from low density to a density higher than  $n_c$  on the ray path in hohlraums. In

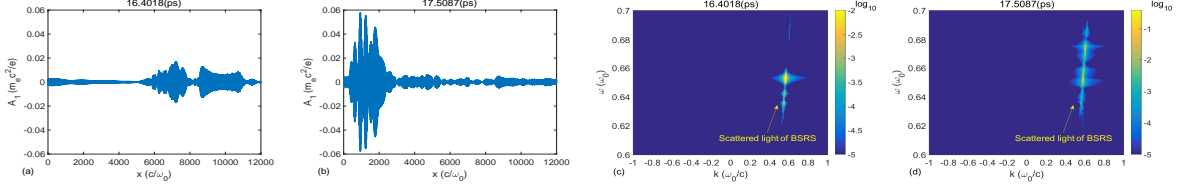


FIG. 5: (Color online) Snapshots of scattered light of SRS at the time about (a,c) 16.4ps and (b,d) 17.5ps in (a,b) real space and (c,d)  $\omega - k$  space for the mobile ions case.

linear theory, low frequency (long wavelength) modes of scattered light of BSRS matched to a high density point (above about  $0.1n_c$ ) should exist and even be stronger. Because the higher density, the higher growth rate and spatial gain for SRS, as long as the high density points exist in the gas region. However, these lower-frequency modes can nevertheless meet their effective quarter critical density points as they propagate to the low density region and have chance to be heavily depleted by re-SRS. While the modes originated from the density points lower than  $0.1n_c$  commonly have the higher frequencies, of which the effective quarter critical density points are higher than  $0.1n_c$ . As a result, these high-frequency (short wavelength) modes have no chance to meet their effective quarter critical density again when propagating to the much lower density region, and would be remained or even be enhanced by re-SRS.

Furthermore, re-SRS would transfer partial energy from BSRS scattered light into its daughter waves. This transferred energy can be deposited quickly in the low density gas plasmas, and has almost no contribution to the conversion into soft X rays. Due to the tiny reflectivity, the rescattered light of re-SRS is hard to be observed directly in the experiments and can not be considered in the hydrodynamic simulation of NIF hohlraums. As a result, this would be a potential reason for the “drive deficit” problem [25]. Experimentally, Thomson Scattering can be used to diagnose the daughter waves of re-SRS [33].

In summary, coupling evolutions of SRS and re-SRS are studied in the indirect drive regime with FLAME code for the first time. Re-SRS is effectively found to be a frequency filter of BSRS light, which heavily depletes the low frequency modes originated from high density points and inflates the high frequency modes generated from low density points, in the typical parameter space which is relevant to the gas-filled hohlraum experiments at NIF. The simulation results reveal the reason why the experimental measured wavelength of BSRS light is always shorter than the simulated results based on the linear theory, and

also partially explain the “energy deficit” appeared in the gas-filled hohlraum experiments at NIF.

This work was supported by Science Challenge Project (Grant No. TZ2016005) and the National Natural Science Foundation of China (Grant No. 11875093 and No. 11775033).

- 
- [1] W. L. Kruer, *The Physics of Laser Plasma Interactions*, Addison-Wesley Publishing Company, 1988.
  - [2] R. S. Craxton, K. S. Anderson, T. R. Boehly, V. N. Goncharov, D. R. Harding, J. P. Knauer, R. L. McCrory, P. W. McKenty, D. D. Meyerhofer, J. F. Myatt, A. J. Schmitt, J. D. Sethian, R. W. Short, S. Skupsky, W. Theobald, W. L. Kruer, K. Tanaka, R. Betti, T. J. B. Collins, J. A. Delettrez, S. X. Hu, J. A. Marozas, A. V. Maximov, D. T. Michel, P. B. Radha, S. P. Regan, T. C. Sangster, W. Seka, A. A. Solodov, J. M. Soures, C. Stoeckl, and J. D. Zuegel, *Phys. Plasmas* **22**, 110501 (2015).
  - [3] E. M. Campbell, V. N. Goncharov, T. C. Sangster, *et al.* *Matter and Radiation at Extremes*, **2**, 37-54 (2017).
  - [4] J. D. Lindl, *Phys. Plasmas* **2**, 3933 (1995).
  - [5] J. D. Lindl, O. Landen, J. Edwards, E. Moses, and NIC Team, *Phys. Plasmas* **21**, 020501 (2014).
  - [6] J. D. Moody, P. Michel, L. Divol, R. L. Berger, E. Bond, D. K. Bradley, D. A. Callahan, E. L. Dewald, S. Dixit, M. J. Edwards, S. Glenn, A. Hamza, C. Haynam, D. E. Hinkel, N. Izumi, O. Jones, J. D. Kilkenny, R. K. Kirkwood, J. L. Kline, W. L. Kruer, G. A. Kyrala, O. L. Landen, S. LePape, J. D. Lindl, B. J. MacGowan, N. B. Meezan, A. Nikroo, M. D. Rosen, M. B. Schneider, D. J. Strozzi, L. J. Suter, C. A. Thomas, R. P. J. Town, K. Widmann, E. A. Williams, L. J. Atherton, S. H. Glenzer and E. I. Moses, *Nature Phys.* **8**, 344, (2012).
  - [7] J. F. Myatt, J. Zhang, R. W. Short, A. V. Maximov, W. Seka, D. H. Froula, D. H. Edgell, D. T. Michel, I. V. Igumenshchev, D. E. Hinkel, P. Michel, and J. D. Moody, *Phys. Plasmas* **21**, 055501 (2014).
  - [8] J. D. Moody, D. A. Callahan, D. E. Hinkel, *et al.*, *Phys. Plasmas* **21**, 056317 (2014).
  - [9] K. Lan, J. Liu, Z. Li, X. Xie, W. Huo, Y. Chen, G. Ren, C. Zheng, D. Yang, S. Li, Z. Yang, L. Guo, S. Li, M. Zhang, X. Han, C. Zhai, L. Hou, Y. Li, K. Deng, Z. Yuan, X. Zhan, F. Wang,

- G. Yuan, H. Zhang, B. Jiang, L. Huang, W. Zhang, K. Du, R. Zhao, P. Li, W. Wang, J. Su, X. Deng, D. Hu, W. Zhou, H. Jia, Y. Ding, W. Zheng, and X. He, *Matter and Radiation at Extremes* **1**, 8 (2016).
- [10] W. Y. Huo, Z. Li, Y. H. Chen, X. Xie, G. Ren, H. Cao, S. Li, K. Lan, J. Liu, Y. Li, S. Li, L. Guo, Y. Liu, D. Yang, X. Jiang, L. Hou, H. Du, X. Peng, T. Xu, C. Li, X. Zhan, Z. Wang, K. Deng, Q. Wang, B. Deng, F. Wang, J. Yang, S. Liu, S. Jiang, G. Yuan, H. Zhang, B. Jiang, W. Zhang, Q. Gu, Z. He, K. Du, X. Deng, W. Zhou, L. Wang, X. Huang, Y. Wang, D. Hu, K. Zheng, Q. Zhu, and Y. Ding, *Phys. Rev. Lett.* **120**, 165001 (2018).
- [11] R. K. Kirkwood, J. D. Moody, J. Kline, E. Dewald, S. Glenzer, L. Divol, P. Michel, D. Hinkel, R. Berger, E. Williams, J. Milovich, L. Yin, H. Rose, B. MacGowan, O. Landen, M. Rosen and J. Lindl, *Plasma Phys. Control. Fusion* **55**, 103001 (2013).
- [12] G. N. Hall, O. S. Jones, D. J. Strozzi, J. D. Moody, D. Turnbull, J. Ralph, P. A. Michel, M. Hohenberger, A. S. Moore, O. L. Landen, L. Divol, D. K. Bradley, D. E. Hinkel, A. J. Mackinnon, R. P. J. Town, N. B. Meezan, L. Berzak Hopkins, and N. Izumi, *Phys. Plasmas* **24**, 052706 (2017).
- [13] D. J. Strozzi, D. S. Bailey, P. Michel, L. Divol, S. M. Sepke, G. D. Kerbel, C. A. Thomas, J. E. Ralph, J. D. Moody, and M. B. Schneider, *Phys. Rev. Lett.* **118**, 025002 (2017).
- [14] D. E. Hinkel, D. A. Callahan, A. B. Langdon, S. H. Langer, C. H. Still, and E. A. Williams, *Phys. Plasmas* **15**, 056314 (2008).
- [15] D. E. Hinkel, M. D. Rosen, E. A. Williams, A. B. Langdon, C. H. Still, D. A. Callahan, J. D. Moody, P. A. Michel, R. P. J. Town, R. A. London, and S. H. Langer, *Phys. Plasmas* **18**, 056312 (2011).
- [16] R. L. Berger, C. A. Thomas, K. L. Baker, D. T. Casey, C. S. Goyon, J. Park, N. Lemos, S. F. Khan, M. Hohenberger, J. L. Milovich, D. J. Strozzi, M. A. Belyaev, T. Chapman, and A. B. Langdon, *Phys. Plasmas* **26**, 012709 (2019).
- [17] P. Michel, W. Rozmus, E. A. Williams, L. Divol, R. L. Berger, R. P. J. Town, S. H. Glenzer, and D. A. Callahan, *Phys. Rev. Lett.* **109**, 195004 (2012).
- [18] P. Michel, L. Divol, R. P. J. Town, M. D. Rosen, D. A. Callahan, N. B. Meezan, M. B. Schneider, G. A. Kyrala, J. D. Moody, E. L. Dewald, K. Widmann, E. Bond, J. L. Kline, C. A. Thomas, S. Dixit, E. A. Williams, D. E. Hinkel, R. L. Berger, O. L. Landen, M. J. Edwards, B. J. MacGowan, J. D. Lindl, C. Haynam, L. J. Suter, S. H. Glenzer, and E. Moses,

- Phys. Rev. E **83**, 046409 (2011).
- [19] D. E. Hinkel, L. F. Berzak Hopkins, T. Ma, J. E. Ralph, F. Albert, L. R. Benedetti, P. M. Celliers, T. Doppner, C. S. Goyon, N. Izumi, L. C. Jarrott, S. F. Khan, J. L. Kline, A. L. Kritcher, G. A. Kyrala, S. R. Nagel, A. E. Pak, P. Patel, M. D. Rosen, J. R. Rygg, M. B. Schneider, D. P. Turnbull, C. B. Yeamans, D. A. Callahan, O. A. Hurricane, Phys. Rev. Lett. **117**, 225002 (2016).
- [20] D. F. DuBois and M. V. Goldman, Phys. Rev. Lett. **14**, 544 (1965).
- [21] D. E. Hinkel, S.W. Haan, A. B. Langdon, T. R. Dittrich, C. H. Still, and M. M. Marinak, Phys. Plasmas **11**, 1128 (2004).
- [22] C. Montes, Phys. Rev. A **31**, 2366 (1985).
- [23] K. Q. Pan, S. E. Jiang, Q. Wang, L. Guo, S. W. Li, Z. C. Li, D. Yang, C. Y. Zheng, B. H. Zhang, and X. T. He, Nucl. Fusion **58**, 096035 (2018).
- [24] B. J. Winjum, J. E. Fahlen, F. S. Tsung, and W. B. Mori, Phys. Rev. Lett. **110**, 165001 (2013).
- [25] S. A. MacLaren, M. B. Schneider, K. Widmann, J. H. Hammer, B. E. Yoxall, J. D. Moody, P. M. Bell, L. R. Benedetti, D. K. Bradley, M. J. Edwards, T. M. Guymmer, D. E. Hinkel, W. W. Hsing, M. L. Kervin, N. B. Meezan, A.S. Moore, and J. E. Ralph, Phys. Rev. Lett. **112**, 105003 (2014).
- [26] J. D. Lindl, P. Amendt, R. L. Berger, S. G. Glendinning, S. H. Glenzer, S. W. Haan, R. L. Kauffman, O. L. Landen, and L. J. Suter, Phys. Plasmas **11**, 339 (2004).
- [27] L. Hao, R. Yan, J. Li W. D. Liu, and C. Ren, Phys. Plasmas **24**, 062709 (2017).
- [28] H. Okuda, J. Comput. Phys. **10**, 475 (1972).
- [29] L. Hao, J. Li, W. D. Liu, R. Yan, and C. Ren, Phys. Plasmas **23**, 042702 (2016).
- [30] J. P. Berenger, J. Comput. Phys. **114**, 185-200 (1994).
- [31] R. Berger, C. Still, E. Williams, and A. Langdon, Phys. Plasmas **5**, 4337 (1998).
- [32] J. Li, R. Yan, and C. Ren, Phys. Plasmas **24**, 052705 (2017).
- [33] S. H. Glenzer, C. A. Back, K. G. Estabrook, R. Wallace, K. Baker, B. J. MacGowan, B. A. Hammel, R. E. Cid and J. S. De Groot, Phys. Rev. Lett. **77**, 1496 (1996).